Received: 4 September 2020 | Accepted: 25 November 2020 | Published online: 17 February 2021

DOI: 10.1002/agj2.20548

Agronomy Journal

ARTICLE

Biometry, Modeling, and Statistics

Simulated climate change effects on soybean production using two crop modules in RZWQM2

L. Ma[1] | Q. X. Fang[2] | M. W. Sima[3] | K. O. Burkey[4] | R. D. Harmel[5]

[1] Rangeland Resources and Systems Research Unit, USDA-ARS, Fort Collins, CO 80526, USA

[2] Agronomy College, Qingdao Agricultural Univ., Qingdao 266109, China

[3] Dep. of Civil and Environmental Engineering, Princeton Univ., Princeton, NJ 08544, USA

[4] Plant Science Research Unit, USDA-ARS, Raleigh, NC 27695, USA

[5] Center for Agricultural Resources Research, USDA-ARS, Fort Collins, CO 80526, USA

Correspondence
Liwang Ma, USDA-ARS, Rangeland Resources and Systems Research Unit, Fort Collins, CO, USA.
Email: Liwang.Ma@usda.gov

Abstract

The ability to predict climate change effects on crop yield through field experiments and crop modeling is essential for developing mitigation strategies. The objective of this study was to compare two different crop modules (CROPGRO and HERMES) in the Root Zone Water Quality Model 2 (RZWQM2) for predicting climate change effects on soybean [*Glycine max* (L.) Merr.] production. The modules were previously calibrated for measured temperature responses using data from a 4-yr open-top chamber experiment (2015–2018) in North Carolina. Both crop modules simulated similar climate change effects in terms of yield and biomass by the end of Year 2100 (2083–2099) using 40 general circulation model (GCM) projections and two Representative Concentration Pathways (RCP4.5 and RCP8.5), compared with the simulations using current baseline (2002–2018). For both modules, much greater reductions in biomass and seed yield were simulated under RCP8.5 than under RCP4.5 due to higher air temperature. In addition, both modules predicted lower variability of biomass and seed yield across these GCMs under irrigated than under rainfed conditions. CROPGRO predicted a greater positive climate change effect in response to the projected higher precipitation and increased atmospheric CO_2 (compared with baseline conditions) than HERMES. Soybean production will likely benefit more from the projected high precipitation and elevated CO_2 under rainfed conditions than under irrigated conditions. Due to much higher simulated yield under irrigation than under rainfed conditions, supplementary irrigation may be an effective mitigation strategy to maintain soybean yield; however, adjusting sowing dates appear to have little effect on soybean production.

1 | INTRODUCTION

Crop models have been used for more than two decades to simulate climate change effects on soybean [*Glycine max* (L.) Merr.] production and develop adaptive strategies (Alexandrov & Hoogenboom, 2000; Lal et al., 1999). In general, elevated high air temperature decreases seed yield and elevated CO_2 in the atmosphere increases soybean yield (Hatfield et al., 2011; Heinemann et al., 2006). One of the most used crop models for such analyses is the Decision Support System for Agrotechnology Transfer (DSSAT)-CROPGRO-Soybean model; however, simulated results are mixed among cultivars and locations (Rolla et al., 2018). In Argentina, Rolla et al. (2018) concluded that soybean yield would increase due to projected high precipitation during growing seasons for

Abbreviations: ET, evapotranspiration; GCM, general circulation model; RCP, Representative Concentration Pathways; RZWQM, Root Zone Water Quality Model; WS, water stress.

RCP4.5 (>32%) and RCP8.5 (>50%) under the near (2015–2039) and the far (2075–2099) future based on the CCSM4 climate model and CROPGRO-Soybean crop model. Lal et al. (1999) also simulated higher soybean yields in future climates due to high CO_2 concentration in the atmosphere and found that an increase of 3 ˚C in air temperature would cancel the "fertilization" effect of doubling CO_2 to 660 ppm in the atmosphere. They also noticed that CO_2 levels would affect photosynthesis more than transpiration due to stomatal closure. Similar soybean responses to climate change were reported by Wang, Qi, Xue, Bukovsky, and Helmers (2015); Bao, Hoogenboom, McClendon, and Urich (2015); and Bao, Hoogenboom, McClendon, & Paz (2015). Relative yield increase was higher under rainfed conditions than under irrigated conditions (Bao, Hoogenboom, McClendon, & Urich, 2015). However, projected crop yield under irrigated conditions had lower annual variability than under rainfed conditions (Ma et al., 2017; Sohoulande, Stone, Szogi, & Bauer, 2019).

On the other hand, Mall, Lal, Bahatia, Rathore, and Singh (2004) predicted that CROPGRO soybean yield would decrease in India at elevated air temperature and doubled CO_2 concentration. Similarly, Carbone et al. (2003) simulated considerable soybean yield decrease in southeastern United States. Also, Eulenstein et al. (2017) stated that soybean yield would decrease in 2071–2100 regardless of climate circulation models (GCMs). These discrepancies in soybean yield responses to climate change may be due to differences in projected temperature and precipitation as well as cultivar parameters (Bao, Hoogenboom, McClendon, & Paz, 2015).

Several research projects have compared soybean models. Battisti, Sentelhas, and Boote (2017) compared five soybean models (FAO-Agroecological Zone; AQUACROP, CROPGRO, APSIM, MONICA) and found that they all predicted similar yields; however, an ensemble of all the models reduced simulation error by half. Later, Battisti et al. (2018) used the ensemble of APSIM, CROPGRO, and MONICA to project climate change effects and identify adaptation strategies to maintain high soybean yield, including supplementary irrigation, advancing sowing date, adopting maturity group close to 8, and increasing plant density to 50 plants m^{-2}. Jing et al. (2017) showed that CROPGRO simulated a 14% increase in soybean yield in the near future (2041–2070) but a decrease in distant future (2071–2100), whereas the STICS model estimated a decrease in both near and distant future under RCP8.5. Wolf (2002a, 2002b) compared CROPGRO and SOYBEANW models for simulated climate change effects after calibration and found that the models responded differently to irrigation management depending on locations. However, in Wolfe et al. (2002a, 2002b) the models were independently applied, thus the results reflected differences not only in crop models but also in other model components such as soil water. Thus improved prediction of soybean production under future climate scenarios is needed to guide management responses.

Core Ideas

- Two crop modules were used to predict climate change effects on soybean.
- Both crop modules simulated similar climate change effects on yield and biomass.
- Greater reductions in biomass/yield were simulated due to higher air temperature.
- CROPGRO predicted a greater positive climate change effect than HERMES.

The most commonly tested adaptation strategies for soybean production are sowing date, cultivar selection, plant density, and irrigation management (Alexandrov & Hoogenboom, 2000; Battisti et al., 2018; Rolla et al., 2018). Sowing date may be delayed (Balvanshi & Tiwari, 2019; Bao, Hoogenboom, McClendon, & Urich, 2015; Mall et al., 2004) or advanced (Battisti et al., 2018; Wolf, 2002a, 2002b) for favorable soybean yield, depending on the location. Selection of crop cultivars for adaptation depends on maturity group but also on irrigation management (Bao, Hoogenboom, McClendon, & Paz, 2015). Irrigation would increase soybean yield compared to rainfed (Wolf, 2002b; Battisti et al., 2018), and increasing plant population would also mitigate the negative effects of high air temperature (Battisti et al., 2018).

Therefore, the objectives of this study were to investigate two soybean modules (CROPGRO and HERMES) in the Root Zone Water Quality Model 2 (RZWQM2) for their ability to simulate climate change effects under irrigated and rainfed conditions from 2083–2099 using 40 GCM projections available for the experimental site and two RCPs (RCP4.5 and RCP8.5) based on previously calibrated model parameters (Sima et al., 2020), and to develop potential mitigation strategies by irrigation and sowing date management by comparing to a 17 yr baseline run from 2002–2018 when measured weather data were available. This study is unique because it is the only one that contains 40 GCM projections and two crop modules and that the plant parameters were calibrated based on experiments at elevated air temperature in open-top chambers.

2 | MATERIALS AND METHODS

2.1 | Model overview

The RZWQM2 is a process-based system model that simulates soil water balance, potential evapotranspiration, soil carbon/nitrogen dynamics, soil heat flux, surface energy balance, soil erosion, and plant growth (Ma et al., 2012). Soil water infiltration during rainfall or irrigation is simulated with the Green–Ampt equation, and water redistribution is calculated by solving the Richards' equation for pressure head. The Brooks–Corey soil water retention curve is used to convert between water pressure head and soil water content. The Shuttleworth–Wallace equation is used to estimate potential evapotranspiration considering crop residue and partial canopy cover effects (Ma et al., 2012). The model contains multiple crop growth modules including the DSSAT suite of crop modules (CROPGRO and CERES) and the HERMES module (Ma, Hoogenboom, Ahuja, Nielsen, & Ascough, 2005; Sima et al., 2020). The CROPGRO has detailed simulation of soybean phenology, yield components, N_2 fixation, and environmental stresses (Boote, Jones, & Hoogenboom, 1998; Jones et al., 2003) and has been evaluated under elevated CO_2 conditions (Alagarswamy, Boote, Allen, & Jones, 2006). HERMES, on the other hand, uses a more simplistic approach and only differentiates among shoots, leaves, roots, and grain (Kersebaum, 1995). The simulated temperature, CO_2, and soil water effects on soybean growth in the two crop modules are provided in Figure 1.

Briefly, leaf photosynthesis in CROPGRO is calculated hourly using the equations tested by Alagarswamy et al. (2006) but scaled up to daily canopy assimilation with the sunlit and shaded approach (Boote & Pickering.,1994; Boote et al., 1998).

$$A = A_{\max}[1 - exp^{-\frac{QE\times PPF}{A_{\max}}}] \tag{1}$$

$$A_{max} = \text{LXREF} \times \text{SLWMAX} \times \text{TEMPMX} \times \text{AGEMXL} \times \text{RE}_{CO2} \tag{2}$$

where A is leaf photosynthesis rate, $A_{\max}$ is the light saturated photosynthesis rate, QE is the quantum efficiency of the leaf, and PPF is photosynthetic photon flux. $A_{\max}$ is estimated from the maximum leaf photosynthesis (LXREF) adjusted by hourly temperature (TEMPMX), leaf nitrogen concentration (AGEMXL), specific leaf weight (SLWMAX), and CO_2 and O_2 factor (RE_{CO2}) (Pickering, Jones, & Boote, 1995).

The HERMES module uses three different algorithms to characterize temperature effects on leaf photosynthesis (Kersebaum, 2013). The Mitchell approach, which was used for this study (Kersebaum & Nendel, 2014; Mitchell et al., 1995) employs a different set of functions for temperature effect. Maximum leaf gross photosynthesis rate ($A_{\max}$) is calculated by:

$$A_{\max} = \frac{(C_i - \Gamma^*)V_{c\max}}{C_i + K_c(1 + O_i/K_o)} \tag{3}$$

$$\Gamma^* = \frac{0.5V_{o\max}K_cO_i}{V_{c\max}K_o} \tag{4}$$

where C_i is the intercellular CO_2 concentration (ppm), Γ^* is the CO_2 photosynthesis compensation point, referring to C_i in the absence of dark respiration, O_i is the intercellular concentration of O_2, $V_{c\max}$ and $V_{o\max}$ (equal to 0.21 of $V_{c\max}$) are the maximum ribulose-1,5-bisphosphate carboxylase-oxygenase (Rubisco)-saturated rate of carboxylation and oxygen, respectively, and K_c and K_o are the Rubisco Michaelis–Menten constants for CO_2 and O_2, respectively. The temperature dependencies of C_i, O_i, K_c, K_o, and $V_{c\max}$ were described by Long (1991).

2.2 | Model calibration

Both CROPGRO-Soybean and HERMES were calibrated with a dataset from an open-top chamber experiment in Raleigh, NC, (35.73° N, 78.69° W) from 2015 to 2018. The top soil contains a 36 cm of sandy loam (fine, kaolinitic, thermic Typic Kanhapludults) with approximately 62% sand, 21% silt, and 17% clay. The underlying deep clay layer (36–100 cm) has 29% sand, 18% silt, and 53% clay (Sima et al., 2020). Irrigation was scheduled to maintain field capacity throughout the growing seasons to minimize water stress. The observed seed yield, biomass, and growth stages from ambient and heated air treatments across the 4 yr were simulated with both the CROPGRO and HERMES crop modules in RZWQM2 that shared the same soil water routine (Sima et al., 2020).

Soil hydraulic parameters were estimated from Rawls, Brakensiek, and Saxton (1982) based on soil texture. The air temperature and humidity measurements were averaged hourly and used as model inputs to quantify weather conditions for each open-top chamber. Additional weather data (hourly rainfall, solar radiation, and wind speed) from 2015 to 2018 were obtained from an on-site weather station. Calibrated crop parameters for both modules are listed in Tables 1 and 2. Across the 4 yr and two treatments, average air temperature was elevated by 3.4–25.7 °C during the growing seasons for the heated treatments compared to the ambient air treatments. As a result, measured average seed yield and final biomass decreased by 22 and 11%, respectively, for the heated treatments, but the elevated air temperature did not significantly affect maturity dates. After calibration at ambient air temperature, both CROPGRO and HERMES were able to simulate yield and biomass reductions in heated treatments. On average, both crop modules simulated lower reduction in seed yield (15% for CROPGRO and 17% for HERMES) compared to experimentally observed 22%. However, simulated reduction in biomass was lower by CROPGRO (7%) than by

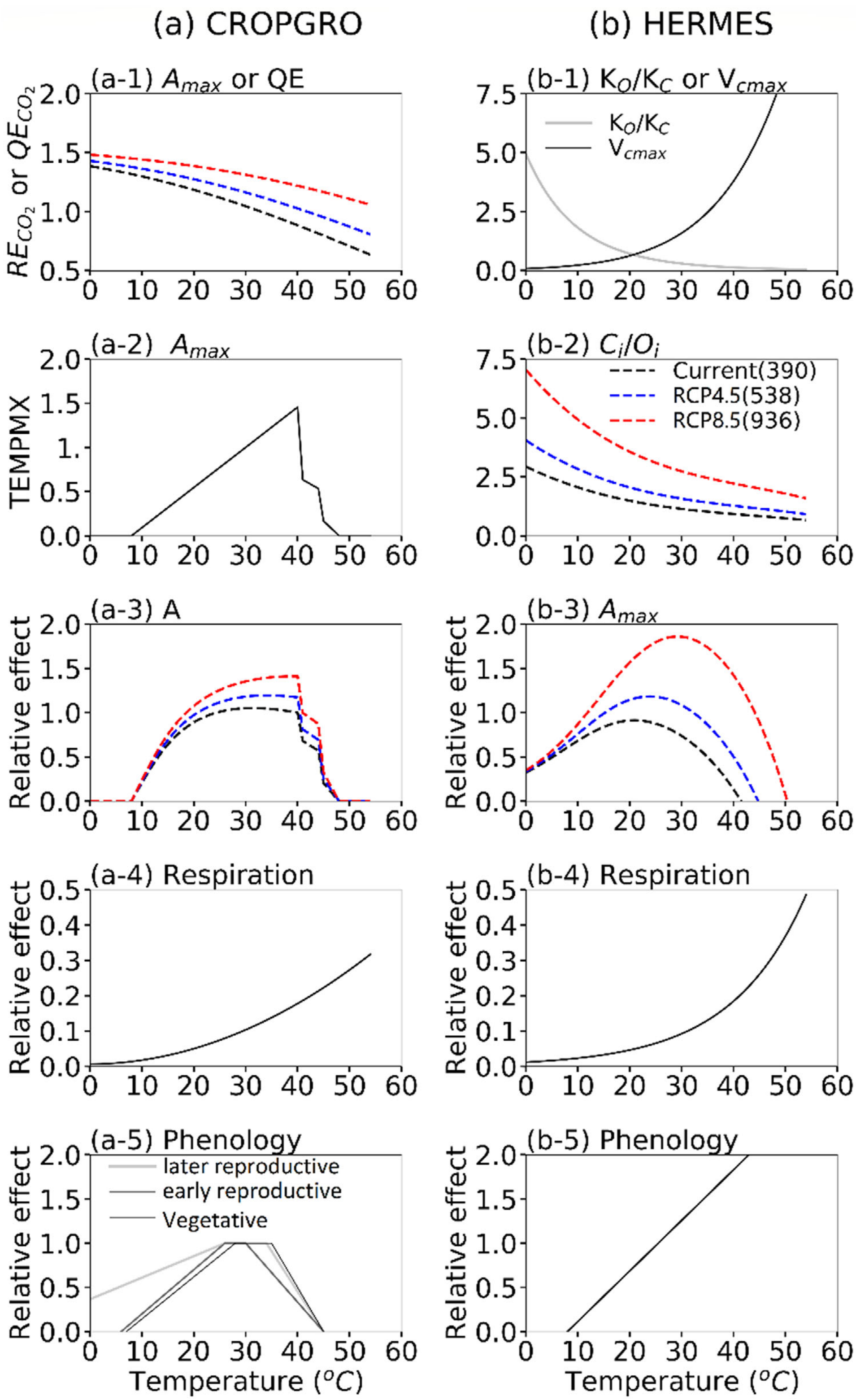

FIGURE 1 Temperature and CO_2 effect (538 ppm for RCP4.5 and 936 ppm for RCP8.5) on leaf photosynthesis, respiration, and growth phenology in (a) CROPGRO and (b) HERMES: (a-1) temperature effects on A_{max} (RE_{CO2}) and QE (QE_{CO2}); (a-2) TEMPMX effect on A_{max}; (a-3) overall temperature and CO_2 effect on A; (a-4) temperature effect on respiration; (a-5) temperature effect on phenology. (b-1) temperature effect on K_o/K_c and V_{cmax}; (b-2) temperature and CO_2 effect on C_i/C_o; (b-3) overall temperature and CO_2 effect on A_{max}; (b-4) temperature effect on respiration; (b-5) temperature effect on phenology (Sima et al., 2020). RCP = Representative Concentration Pathways, RE = CO_2 factor to leaf quantum efficiency, QE = quantum efficiency

TABLE 1 Calibrated soybean cultivar parameters in CROPGRO-Soybean. (Sima et al., 2020)

Parameter	Values
CSDL: Critical Short Day Length below which reproductive development progresses with no daylength effect (for short day plants) (hour)	12.8
PPSEN: Slope of the relative response of development to photoperiod with time (positive for short-day plants) (1/hour)	0.27
EM-FL: Time between plant emergence and flower appearance (R1) (photothermal days)	23.3
FL-SH: Time between first flower and first pod (R3) (photothermal days)	10.0
FL-SD: Time between first flower and first seed (R5) (photothermal days)	15.6
SD-PM: Time between first seed (R5) and physiological maturity (R7) (photothermal days)	45.0
FL-LF: Time between first flower (R1) and end of leaf expansion (photothermal days)	17.1
LFMAX: Maximum leaf photosynthesis rate at 30 ˚C, 350 ppm CO_2, and high light, mg CO_2/m^2*s	2.4
SLAVR: Specific leaf area of cultivar under standard growth conditions, $cm^2\ g^{-1}$	300
SIZLF: Maximum size of full leaf (three leaflets), cm^2	250
XFRT: Maximum fraction of daily growth that is partitioned to seed + shell	0.90
WTPSD: Maximum weight per seed, 10^{-3} kg	0.19
SFDUR: Seed-filling duration for pod cohort at standard growth conditions (photothermal days)	32.1
SDPDV: Average seeds per pod under standard growing conditions (no. pod^{-1})	2.5
PODUR: Time required for cultivar to reach final pod load under optimal conditions (photothermal days)	17.8

TABLE 2 Calibrated soybean parameters (only development phase thermal time was adjusted in parenthesis from the default values) in the HERMES model[a]. (Sima et al., 2020)

Growth phases	1	2	3	4	5	6	7
Development phase thermal time, ˚C day	88	150	568	220	470	550	25
Base temperature, ˚C	8	8	6	6	6	0	9
Day length requirements, hour	0	−12.8	−12.8	−12.8	−12.8	−12.8	0
Base day length in phase, hour	0	−22.35	−22.35	−22.35	−22.35	−22.35	0
Specific leaf area, $m^2\ m^{-2}\ kg^{-1}$ (10^{-3})	1.66	1.73	2.16	2.00	1.41	2.0	2.0
Partitioning of photosynthate to roots	0.5	0.2	0.13	0.1	0	0	0
Partitioning of photosynthate to leaves	0.5	0.6	0.33	0.4	0	0	0
Partitioning of photosynthate to stems	0	0.2	0.54	0.5	0	0	0
Partitioning of photosynthate to ears	0	0	0	0	1	1	0
Leaf death rate	0	0	0	0	0.05	0.05	0.05
Root N content	0.02	0.012	0.01	0.01	0.01	0.01	0.01

[a]The negative values for day length requirements and base day length in phase suggest that phenological development is delayed when days become too long.

HERMES (20%), with an ensemble reduction of 13% that was close to observed 11% decrease. CROPGRO simulated maturity dates were closer to experimental results than that of HERMES. The latter advanced soybean maturity dates by as many as 19 d at high air temperature. Across the 4 yr and two treatments, simulation error (root mean square error, RMSE) for seed yield was 971 kg ha^{-1} by CROPGRO and 814 kg ha^{-1} by HERMES, and that for biomass was 1,609 kg ha^{-1} for CROPGRO and 1,631 kg ha^{-1} for HERMES. Other details and statistics on model calibration are available in Sima et al. (2020).

2.3 | Baseline and climate change scenarios

Long-term weather data including daily solar shortwave radiation, maximum and minimum air temperature, wind speed, relative humidity, and precipitation, were obtained from the State Climate Office of North Carolina (http://climate.ncsu.edu/cronos/). We were only able to obtain quality controlled data from 2002 to 2018, which served as our baseline for climate change simulation. Missing solar radiation was estimated from a nearby weather station at Clayton, NC (about 22 km Southeast of Raleigh, NC). The baseline simulations

TABLE 3 The 40 general circulation model (GCM) projections used in this study and their originating institutions (Brekke et al., 2013; Pierce et al., 2015)

GCM acronym	GCM source/institution
ACCESS1.0	Commonwealth Scientific and Industrial Research Organisation (CSIRO) and Bureau of Meteorology, Australia
BCC_CSM1.1	Beijing Climate Center, China
CanESM2 (1…5)[a]	Canadian Centre for Climate Modelling and Analysis, Canada
CCSM4 (1…2)	National Center for Atmospheric Research (NCAR), USA
CESM1[biogeochemistry (BGC)]	NCAR, USA
CNRM-CM5	Centre National de Recherches Météorologiques, France
CSIRO Mk3.6.0 (1…10)	Queensland Climate Change Centre of Excellence and CSIRO, Australia
GFDL-ESM2G	Geophysical Fluid Dynamics Laboratory (GFDL), Princeton, NJ
GFDL-ESM2M	GFDL, Princeton, NJ
INM-CM4	Institute of Numerical Mathematics, Russian Academy of Sciences, Russia
IPSL-CM5A-LR (1…4)	L'Institut Pierre-Simon Laplace, France
IPSL-CM5A-MR	L'Institut Pierre-Simon Laplace, France
MIROC-ESM	Japan Agency for Marine-Earth Science and Technology (JAMSTEC) and National Institute for Environmental Studies (NIES), Japan
MIROC-ESM-CHEM	JAMSTEC and NIES, Japan
MIROC5 (1…3)	Atmosphere and Ocean Research Institute and NIES, Japan
MPI-ESM-LR (1…3)	Max Planck Institute for Meteorology, Germany
MPI-ESM-MR	Max Planck Institute for Meteorology, Germany
MRI-CGCM3	Meteorological Research Institute, Japan
NorESM1-M	Norwegian Climate Centre, Norway

[a]Multiple simulation runs with different initial conditions.

were run from 2002 to 2018 under rainfed and irrigated (no water stress) conditions, separately.

Bias-corrected and spatially disaggregated (BCSD) projections from the World Climate Research Program's (WCRP) coupled model inter-comparison project phase 5 (CMIP5) were obtained from http://gdo-dcp.ucllnl.org/downscaled_cmip3_projections/ to generate 40 GCM projections (Table 3) for two commonly studied Representative Concentration Pathways (RCP) (RCP4.5 and RCP8.5) by the end of Year 2100 (Brekke, Thrasher, Maurer, & Pruitt, 2013; Pierce, Cayan, Maurer, Abatzoglou, & Hegewisch, 2015). Each projection included maximum and minimum air temperature and precipitation from 2083 to 2099, which was then superimposed onto the historical weather data of wind speed, relative humidity, and solar radiation from 2002 to 2018. By the end of 2100, atmospheric CO_2 concentration was estimated to be 538 ppm under RCP4.5 and 936 ppm under RCP8.5 (Fu, Ha, & Ko, 2016; IPCC, 2014; Meinshausen et al., 2011).

The projected changes in precipitation, and maximum and minimum air temperature from 2083 to 2099 under RCP4.5 and RCP8.5 are shown in Figure 2. Precipitation was projected to increase by 22% on average for both RCP4.5 and RCP8.5, where large increases occurred mainly in January–March and July–August (Figure 2). Minimum and maximum air temperature was projected to increase by 2.2 and 2.8 ˚C for RCP4.5, and 4.6 and 4.5 ˚C for RCP8.5, respectively. Most GCM models projected similar temperature increase among different months for RCP4.5 and higher temperature increase in May–October than in other months for RCP8.5 (Figure 2b, 2c). Both CROPGRO and HERMES in RZWQM2 were run for each of the 40 GCM projections without/with elevated CO_2 concentration (i.e., maintaining at 395 ppm without elevated CO_2, increasing to 538 ppm and 936 ppm by 2100 for RCP4.5 and RCP8.5, respectively) under both rainfed and irrigated conditions, resulting in 320 climate change scenarios (2 × 2 × 2 × 40) for each crop module.

Since the downscaled GCM projections for air temperature and precipitation were used directly without further adjustment to the specific local weather station, these projections could be biased for the particular location in this study, depending on the weather station and methods used for BCSD in the climate database (Sohoulande & Singh, 2016; Sohoulande et al., 2019). However, since our goal was mainly to compare two crop modules in simulating elevated temperature effects on soybean production in combination with elevated CO_2 and irrigation, such a potential bias would not affect our results and conclusion, especially when the baseline and GCM projections represent the general trends in climate change in the region. The validity of using the downscaled weather data directly was checked by comparing measured

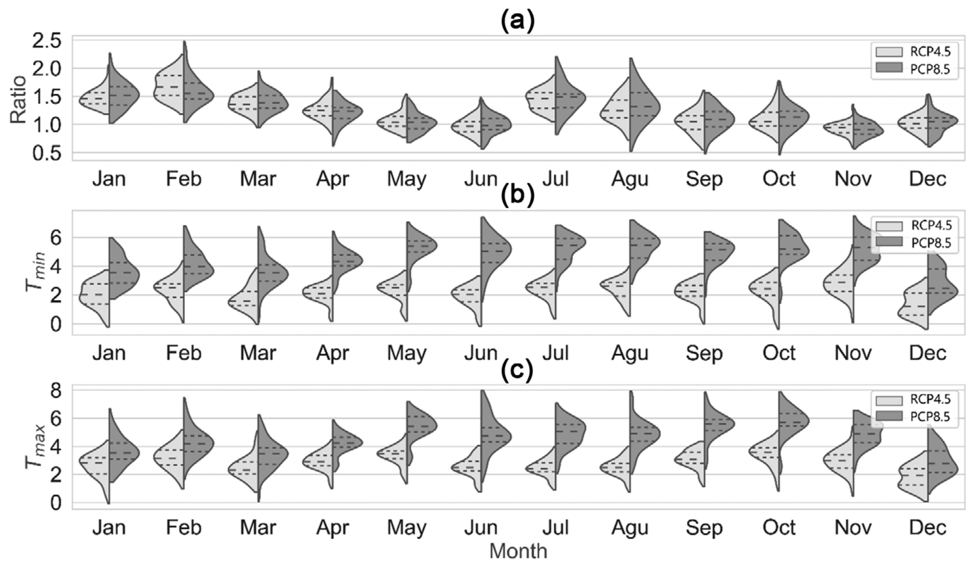

FIGURE 2 Violin distributions for projected changes in monthly precipitation (ratio of general circulation models [GCMs] to current), minimum air temperature (T_{min}, ˚C), and maximum air temperature (T_{max}, ˚C) from the 40 GCM projections under RCP4.5 and RCP8.5 compared with the current climate condition at Raleigh, NC. The three inside lines from bottom to top of violins represent the 25th, 50th, and 75th percentiles across the 40 GCM projections, respectively. RCP = Representative Concentration Pathways

and GCM projected weather data for Years 2002–2018. The average GCM projected maximum and minimum temperature was 22.48 and 10.88 ˚C for 2002–2018, respectively, which was close to the measured averages of 22.01 and 10.72 ˚C, respectively. Projected average annual rainfall was 119 cm, which was also close to measured 109 cm. Therefore, the GCM projections should be reasonable for the location. Additionally, selecting 17 yr (2083–2099) out of the 98 yr (2002–2099) of GCM projections at the end of the century would represent a climate variability and worst scenario of agronomic interest for management and mitigation.

3 | RESULTS

3.1 | Baseline simulations under rainfed and irrigated conditions

Under rainfed condition (Figure 3a), average annual simulated final biomass for 2002–2018 was slightly lower for CROPGRO (8,093 ± 2,718 kg ha^{-1}) than for HERMES (8,895 ± 2,061 kg ha^{-1}). CROPGRO simulated more than 6,588 kg ha^{-1} of biomass in 75% of the years, while the 75th percentile for HERMES was 8,451 kg ha^{-1} (Table 4, Figure 3). Simulated biomass with irrigation (no water stress) was also similar between the two modules, with average values of 14,011 ± 973 kg ha^{-1} for CROPGRO and 12,329 ± 931 kg ha^{-1} for HERMES (Figure 3).

While predicted biomass was very similar, average CROPGRO-simulated seed yield (2,827 ± 1,562 kg ha^{-1}) was only 52% of that simulated by HERMES (5,416 ± 1,516 kg ha^{-1}) under rainfed conditions (Table 4, Figure 4). Across the 17 yr, CROPGRO predicted seed yield below 3,521 kg ha^{-1} in 75% of the years, while the 75th percentile for HERMES was 4,550 kg ha^{-1} (Figure 4). Under irrigated conditions, CROPGRO again simulated lower seed yield (6,276 ± 797 kg ha^{-1}) than HERMES (7,416 ± 701 kg ha^{-1}). CROPGRO simulated seed yield lower than 6,305 kg ha^{-1} in 75% of years, while the 75th percentile for HERMES 7,330 kg ha^{-1} (Figure 4).

With adequate irrigation, both modules simulated relatively stable soybean biomass and yield with coefficient of variation (CV) values below 13% across the 17 yr. Under rainfed conditions, CROPGRO simulated greater year-to-year variability in both biomass (CV = 34%) and seed yield (CV = 55%) than HERMES (CV = 23% for biomass; CV = 28% for yield) (Figures 3 and 4). The lower seed yield simulated by CROPGRO was partially due to the higher sensitivity to water stress in CROPGRO, since the modules produced very similar crop water stress predictions (Figure 4, Table 4). This discrepancy may be explained by the fact that CROPGRO simulated soybean seed yield using more complex physiological processes with high sensitivity to water stresses, such as accounting for yield components of seed number and seed weight.

Average simulated physiological maturity date from 2002 to 2018 was 140 d after planting by CROPGRO and 127 d after planting by HERMES, which were comparable with that simulated ones for the unheated experimental treatments from 2015 to 2018 (126 d after planting for CROPGRO and 124 d after planting for HERMES, Table 4) regardless of rainfed and irrigated conditions (Sima et al., 2020). HERMES-predicted physiological maturity dates showed high variation [standard deviation (SD) = 8 d] across the 17 yr under

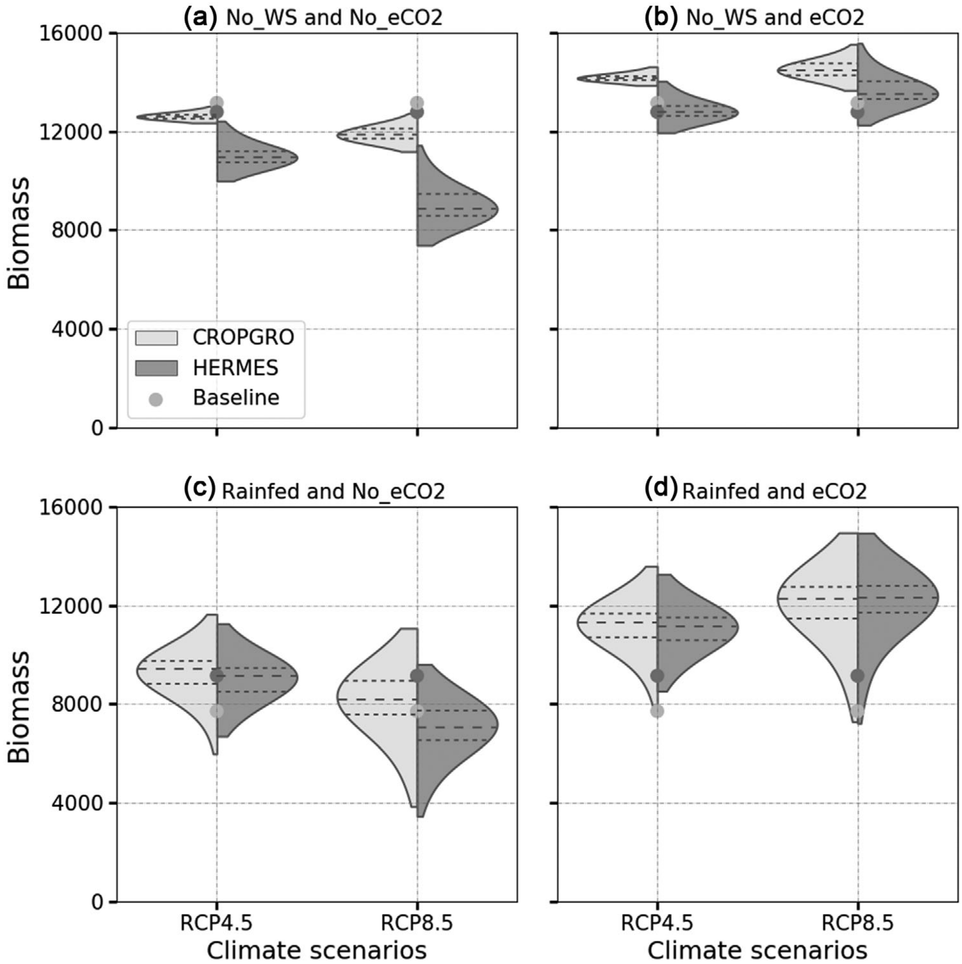

FIGURE 3 Violin distributions of simulated average soybean biomass (kg ha^{-1}) from 2083 to 2099 for the 40 general circulation model [GCM] projections by CROPGRO (light gray) and HERMES (gray) in response to combined factors of water stress ([a and b] Irrigated [No_WS] and [c and d] Rainfed), temperature increase (2.5 ˚C for RCP4.5 and 4.5 ˚C for RCP8.5) and CO_2 levels (current CO_2 level: [a and c] No_eCO_2, [b and d] elevated CO_2 levels of 538 ppm for RCP4.5 and 936 ppm for RCP8.5: eCO_2). The baseline (dots) was averaged from the simulated soybean biomass under current climate conditions from 2002 to 2018 with CO_2 level of 395 ppm in Raleigh, NC. The three inside lines from bottom to top of violins represent the 25, 50, and 75th percentiles across the 40 GCM projections, respectively. Legend is applicable to all plots. RCP = Representative Concentration Pathways

both rainfed and irrigated conditions (Table 4), however, CROPGRO, showed lower variation under irrigated conditions (SD = 1.7 d) than under rainfed conditions (SD = 6.9 d), indicating a higher sensitivity of CROPGRO-simulated soybean maturity dates to water stress (Ruiz-Nogueira, Boote, & Sau, 2001).

3.2 | Projected climate change simulation under irrigated conditions

Without elevated CO_2 concentration, both modules simulated decreases in biomass and yield with much more deduction under RCP8.5 than under RCP4.5, and more reduction simulated by HERMES than by CROPGRO (Table 4). Under RCP4.5, CROPGRO simulated −3.3 and −5.1% reduction in biomass and yield, respectively, whereas HERMES simulated −11.1 and −12.7% reduction in biomass and yield, respectively. Under RCP8.5, the corresponding percentages were −8.8 and −17.3% by CROPGRO, and −24.2 and −26.1% by HERMES, compared to the irrigated baseline scenarios. These reductions occurred in almost all 40 GCM projections, where more reduction in biomass and seed yield was simulated by HERMES (14–30%) than by CROPGRO (4–17%) (Table 4, Figures 3 and 4). The simulated long-term reduction was comparable with the experimental results from 2015 to 2018 (11% for biomass and 22% for seed yield) (Sima et al., 2020).

With elevated CO_2 concentration under both RCP4.5 and RCP8.5, both modules simulated slightly higher average soybean biomass (1.5–10%, Figure 3) and seed yield (0–9%, Figure 4) under irrigated conditions, compared with the

TABLE 4 Simulated average soybean biomass (kg ha^{-1}), seed yield (kg ha^{-1}), and growth duration (GD, days) and average daily crop water stress index (WS, higher value means less water stress) for current climate (2002–2018, normal temperature (T) and CO_2 concentration [CO_2]) and further climate changes of Representative Concentration Pathways, RCP4.5 and RCP 8.5, with or without CO_2 elevations by CROPGRO and HERMES modules under rainfed and irrigated conditions (standard deviation [SD] was calculated based on the 2002–2018 current climate simulation or across these 40 general circulation model [GCM] projections, respectively, for RCP4.5 or RCP8.5)

Climate scenario	T/CO_2 increase	Water	Crop module	Biomass (mean ± SD)	Yield (mean ± SD)	GD (mean ± SD)	WS (mean ± SD)
Baseline	Normal	Irrigated	CROPGRO	14,011 ± 973	6,276 ± 797	141 ± 1.7	1.0 ± 0.0
			HERMES	12,329 ± 931	7,416 ± 701	127 ± 8.0	1.0 ± 0.0
		Rainfed	CROPGRO	8,093 ± 2718	2,827 ± 1562	140 ± 6.9	0.82 ± 0.10
			HERMES	8,895 ± 2061	5,416 ± 1516	127 ± 8.0	0.82 ± 0.10
RCP4.5	Increased T only	Irrigated	CROPGRO	13,540 ± 881	5,957 ± 551	137 ± 1.4	1.0 ± 0.0
			HERMES	10,956 ± 826	6,469 ± 612	112 ± 4.1	1.0 ± 0.0
		Rainfed	CROPGRO	9,620 ± 2297	3,381 ± 1578	134 ± 4.7	0.88 ± 0.08
			HERMES	8,874 ± 1689	5,048 ± 1200	112 ± 4.1	0.88 ± 0.08
	Increased T and CO_2	Irrigated	CROPGRO	15,180 ± 1007	6,833 ± 647	137 ± 1.4	1.0 ± 0.0
			HERMES	12,517 ± 904	7,418 ± 701	112 ± 4.1	1.0 ± 0.0
		Rainfed	CROPGRO	11,719 ± 2357	4,384 ± 1793	134 ± 4.5	0.90 ± 0.07
			HERMES	10,677 ± 1733	6,152 ± 1311	112 ± 4.1	0.90 ± 0.08
RCP8.5	Increased T only	Irrigated	CROPGRO	12,768 ± 938	5,187 ± 724	139 ± 2.2	1.0 ± 0.0
			HERMES	9,347 ± 934	5,480 ± 641	101 ± 4.2	1.0 ± 0.0
		Rainfed	CROPGRO	8,343 ± 2410	2,488 ± 1486	135 ± 5.0	0.84 ± 0.08
			HERMES	7,145 ± 1804	4,057 ± 1195	101 ± 4.2	0.86 ± 0.09
	Increased T and CO_2	Irrigated	CROPGRO	15,481 ± 1140	6,527 ± 920	139 ± 2.2	1.0 ± 0.0
			HERMES	13,098 ± 1083	7,747 ± 860	101 ± 4.2	1.0 ± 0.0
		Rainfed	CROPGRO	12,404 ± 2545	4,372 ± 1938	136 ± 4.5	0.90 ± 0.07
			HERMES	11,427 ± 1971	6,629 ± 1526	101 ± 4.2	0.90 ± 0.03

irrigated baselines. Therefore, soybean production is predicted to be maintained under irrigated condition in the future, regardless of RCPs. These results indicated that, in spite of projected higher air temperature increase under RCP8.5 (4.5 ˚C), the projected higher CO_2 concentration (936 ppm) still offset the more negative effects of high temperature on soybean compared to simulations under RCP4.5 (538 ppm and 2.5 ˚C increase). Comparing the two modules, the CROPGRO produced slightly higher increase in biomass (8–10% vs. 1–6%) and yield (4–9% vs. 0–4%) from their baselines under RCP4.5 and RCP8.5 (Table 4).

A further analysis of annual yield and biomass in response to climate change (averaged from the 40 GCM projections) was presented using cumulative distribution functions (CDF) in Figures 5 and 6. Under no water stress (fully irrigated) conditions, more increases in biomass (Figure 5) and seed yield (Figure 6) were simulated across the 17 yr by the two modules with CO_2 elevation for RCP8.5 than for RCP4.5, compared with their respective 2002–2018 baselines. HERMES generally produced lower biomass but higher seed yield than CROPGRO across the 17 yr under the same climate change scenarios, which was consistent across the 40 GCM projections (Figures 3 and 4).

The simulated growing season evapotranspiration (ET) generally increased from the baselines for most (>90%) GCMs (Figure 7), but less increase in ET was simulated by the two modules with elevated CO_2 than without elevated CO_2, which could be due to CO_2–induced stomatal closure (Islam, Ahuja, Garcia, Ma, & Saseendran, 2012; Lal et al., 1999; Wang et al., 2015). The increased ET with no water stress and under baseline CO_2 levels was mainly associated with the increased air temperature (Figure 7). The higher ET simulated by the two modules under RCP4.5 and RCP8.5 suggested that air temperature had more impact on ET than CO_2. On the other hand, the slightly lower simulated ET under RCP8.5 than RCP4.5 indicated that CO_2 effects on stomatal closure partially offset the air temperature effect on ET. Although CROPGRO predicted slightly lower ET than HERMES, both modules produced very similar ET responses to increase in air temperature and CO_2 under the RCP4.5 and RCP8.5 pathways (Figure 7).

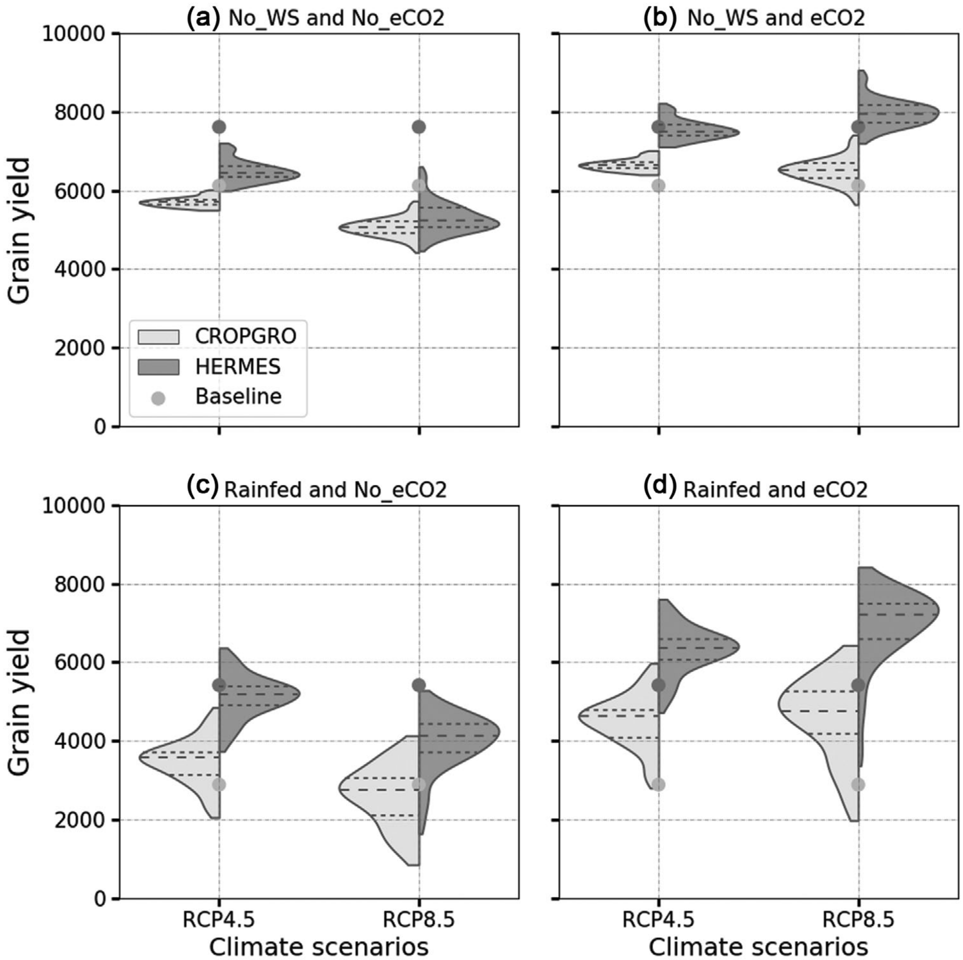

FIGURE 4 Violin distributions of simulated average soybean yield (kg ha^{-1}) from 2083 to 2099 for the 40 general circulation model (GCM) projections by CROPGRO (light gray) and HERMES (gray) in response to combined factors of water stress ([a and b] No_WS and [c and d] Rainfed), temperature increase (2.5 ˚C for RCP4.5 and 4.5 ˚C for RCP8.5) and CO_2 levels (current CO_2 level: [a and c] No_eCO_2, [b and d] elevated CO_2 levels of 538 ppm for RCP4.5 and 936 ppm for RCP8.5: eCO_2). The baseline (dots) was averaged from the simulated soybean biomass under current climate condition from 2002 to 2018 with CO_2 level of 395 ppm in Raleigh, NC. (The three insider lines from bottom to top in violins present the 25th, 50th, and 75th percentiles across the 40 GCM projections, respectively). Legend is applicable to all plots. RCP= Representative Concentration Pathways

No significant effects of elevated CO_2 concentration on soybean maturity were simulated by both modules (Table 4). HERMES simulated much earlier maturity dates than CROPGRO under both RCP4.5 (Δ = 15 vs. 2 d) and RCP8.5 (Δ = 26 vs. 4 d), compared with their respective baselines (Table 4, Figure 8). The average soybean maturity date simulated by CROPGRO was 137 and 139 d after planting for RCP4.5 and RCP8.5, respectively, compared to 112 d after planting and 101 d after planting by HERMES (Table 4). Across the 40 GCM projections, HERMES-simulated maturity date showed greater variation (SD = 4 d) CROPGRO (SD = 2). Crop water stress showed no significant effects on simulated soybean maturity by HERMES, while CROPGRO predicted that maturity dates were 3–4 d later under irrigated than rainfed conditions.

3.3 | Projected climate change simulation under rainfed conditions

Without elevated CO_2 concentration, CROPGRO simulated a 19% increase in both average biomass and average yield under RCP4.5 due to a 22% increase in projected precipitation from 2083 to 2099, as influenced by the lower predicted crop water stress (WS) for the GCMs (average WS = 0.86–0.90) than for the baselines (average WS = 0.82; Table 4, Figures 3 and 4). Under RCP8.5, CROPGRO simulated a 3% increase in biomass but a −12% decrease in yield. On the other hand, HERMES simulated decreases in both biomass and yield under both RCPs with −0.2% reduction in biomass and −6.7% reduction in yield under RCP4.5 and −19.6 and −25.1% reductions under RCP8.5, compared with the rainfed baselines. These trends were consistent among almost all

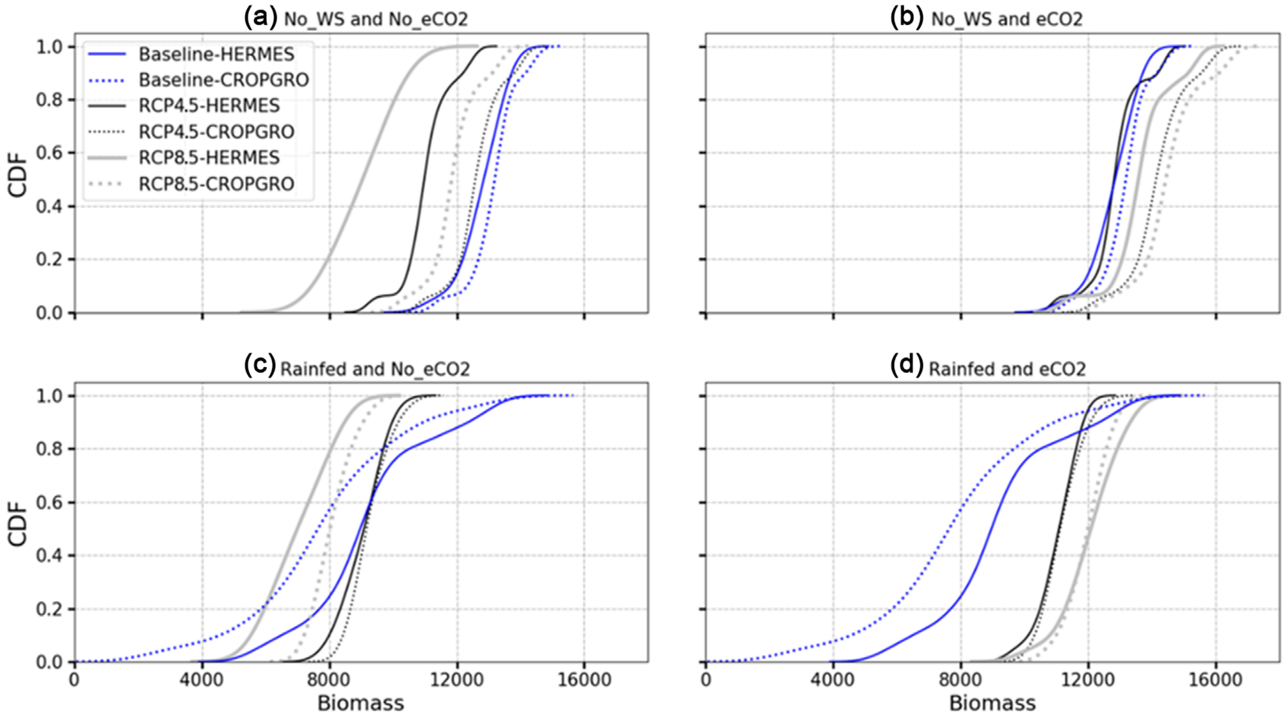

FIGURE 5 Cumulative distribution function (CDF) of simulated average soybean biomass (kg ha^{-1}) from the 40 general circulation model (GCM) projections across 2002 to 2018 by CROPGRO (solid lines) and HERMES (dot lines) in response to combined factors of water stress ([a and b] No_WS [Irrigation], and [c and d] Rainfed), temperature increase (2.5 ˚C for RCP45 and 4.5 ˚C for RCP85) and CO_2 levels (current CO_2 level [a and c]: No_eCO_2, [b and d] elevated CO_2 levels of 538 ppm for RCP4.5 and 936 ppm for RCP8.5: eCO_2). The baselines (blue lines) was obtained from the simulated biomass under current climate condition from 2002 to 2018 with CO_2 level of 395 ppm. Legend is applicable to all plots. RCP = Representative Concentration Pathways

the 40 GCM projections, where more reduction in biomass and seed yield was simulated by HERMES (−14 to −30%) than by CROPGRO (−4 to −17%) under both RCP4.5 and RCP8.5.

With elevated CO_2 concentration under RCP4.5 and RCP8.5, both modules simulated higher average soybean biomass (20–44%, Figure 3) and seed yield (13–55%, Figure 4) for rainfed conditions compared with the rainfed baselines, which was higher than that under irrigated conditions (0–10%), compared with their respective baselines without CO_2 elevations (Figures 3 and 4). These results showed more compensation effects from elevated CO_2 concentration for soybean reduction due to increased air temperature under rainfed conditions than under irrigated conditions. Under rainfed conditions, CROPGRO predicted much greater increase in biomass (50 vs. 26%) and yield (55 vs. 22%) than HERMES (Table 4). Both modules simulated higher increase in average biomass and yield for RCP8.5 than for RCP4.5 under both rainfed (54 vs. 24%) and irrigated conditions (8 vs. 5%). These results indicated that, in spite of projected higher air temperature increase for RCP8.5 (4.5 ˚C), the projected higher CO_2 concentration (936 ppm) still offset the negative effects of high temperature relative to RCP4.5 (538 ppm and 2.5 ˚C increase).

As shown in Figures 5 and 6, under rainfed conditions without elevated CO_2, the simulated biomass and seed yield were reduced due to increased air temperature (RCP4.5 and PCP8.5) in wet years but were increased by the projected higher precipitation (Figure 3) in dry years. When CO_2 concentration was elevated, the simulated biomass and seed yield were slightly reduced in a few years (<20%) when projected precipitation was low, but they were significantly increased in other years (>80%) due to the combined effects of increased CO_2 and precipitation.

As expected, simulated seasonal evapotranspiration (ET) was generally lower under rainfed conditions (Figure 7) than that under irrigated conditions in both modules and under both RCPs. The increased ET under rainfed conditions was mainly associated with increased precipitation and air temperature under RCP4.5 and RCP8.5 (Figure 3) compared to the rainfed baselines. Although both modules simulated similar ET and ET responses to increased air temperature and CO_2 under RCP4.5 and RCP.8.5, CROPGRO predicted lower transpiration but higher evaporation than HERMES. HERMES transpiration predictions were higher mainly due to higher simulated leaf area index in the growing seasons than CROPGRO, which allowed less partitioning of total potential ET into potential surface evaporation.

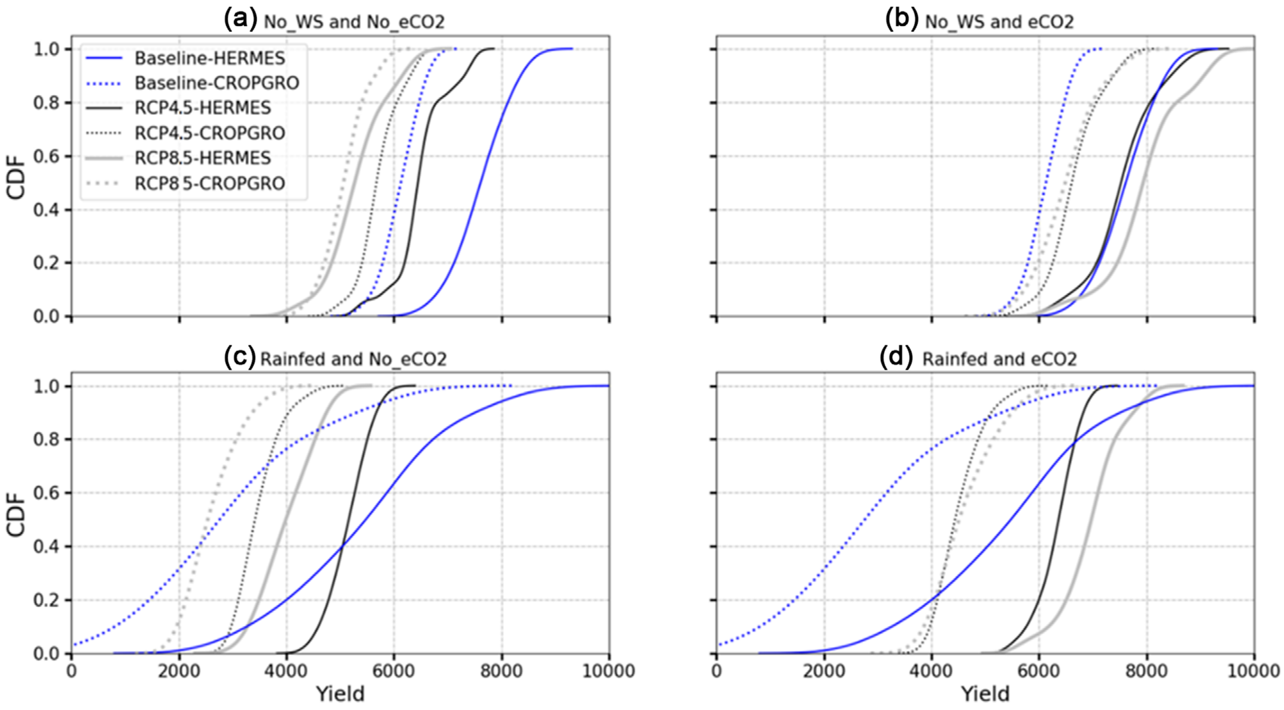

FIGURE 6 Cumulative distribution function (CDF) of simulated average soybean seed yield (kg ha^{-1}) from the 40 general circulation model (GCM) projections across 2002 to 2018 by CROPGRO (solid lines) and HERMES (dot lines) in response to combined factors of water stress ([a and b]No_WS [Irrigation], a and b, and [c and d] Rainfed), temperature increase (2.5 ˚C for RCP4.5 and 4.5 ˚C for RCP8.5) and CO_2 levels (current CO_2 level: [a and c] No_eCO_2, [b and d] elevated CO_2 levels of 538 ppm for RCP4.5 and 936 ppm for RCP8.5: eCO_2). The baselines (blue lines) was obtained from the simulated biomass under current climate condition from 2002 to 2018 with CO_2 level of 395 ppm. Legend is applicable to all plots. RCP = Representative Concentration Pathways

4 | DISCUSSION

Although both modules were calibrated and validated with experimental data from 2015 to 2018, there were considerable differences between the two using historical data from 2002 to 2018 under irrigated conditions. Compared to experimental averages under ambient air temperature, CROPGRO simulated 17% higher biomass and 7% lower yield, whereas HERMES simulated almost the same biomass but 10% higher yield in 2002–2018 baseline runs. The differences were magnified under rainfed conditions with CROPGRO simulating less than half of the irrigated yield (55% reduction) and HERMES simulating only 27% reduction. Therefore, caution should be taken in interpreting projected soybean yield under rainfed conditions as no experimental results were available under rainfed conditions to validate either module. However, the responses of both modules to climate change should be valid, as they agree with literature values (Bao, Hoogenboom, McClendon, & Urich, 2015; Bao, Hoogenboom, McClendon, & Paz, 2015).

Projected climate change effects on soybean growth and phenology differed greatly between irrigation and rainfed conditions in both modules. The changes in soybean response to climate change was larger under rainfed conditions than under irrigated conditions due to a projected 22% increase in precipitation (Figure 2a) and increased CO_2 by Year 2100. Similar results were reported by Alexandrov, Eitzinger, Cajic, and Oberforster (2002), who using CROPGRO in Austria, found that warming temperature in combination with increased precipitation would increase soybean yield. However, a drier climate in the future would limit the benefit from CO_2 elevation and reduce soybean yield, as reported for the U. S. Midwest (Jin, Ainsworth, Leakey, & Lobell, 2018; Schauberger et al., 2017). The positive effect of CO_2 elevation also compensated more for the negative effect of temperature increase under rainfed conditions than irrigation conditions (Table 4, Figures 3 and 4).

Although the CROPGRO and HERMES modules use different CO_2 assimilation algorithms and temperature response functions (Figure 1; Sima et al., 2020), both produced similar responses of soybean yield to climate change scenarios under RCP4.5 and RCP8.5 (Figures 3 and 4), which was consistent with previous results on evaluating several CO_2 assimilation algorithms with FACE experiments (Nendel et al., 2009). Under rainfed conditions, however, CROPGRO simulated greater climate change effects on seed yield and biomass than HERMES under both RCP4.5 (50 vs. 26%) and RCP8.5 (55 vs. 22%), indicating greater sensitivity of CROPGRO to

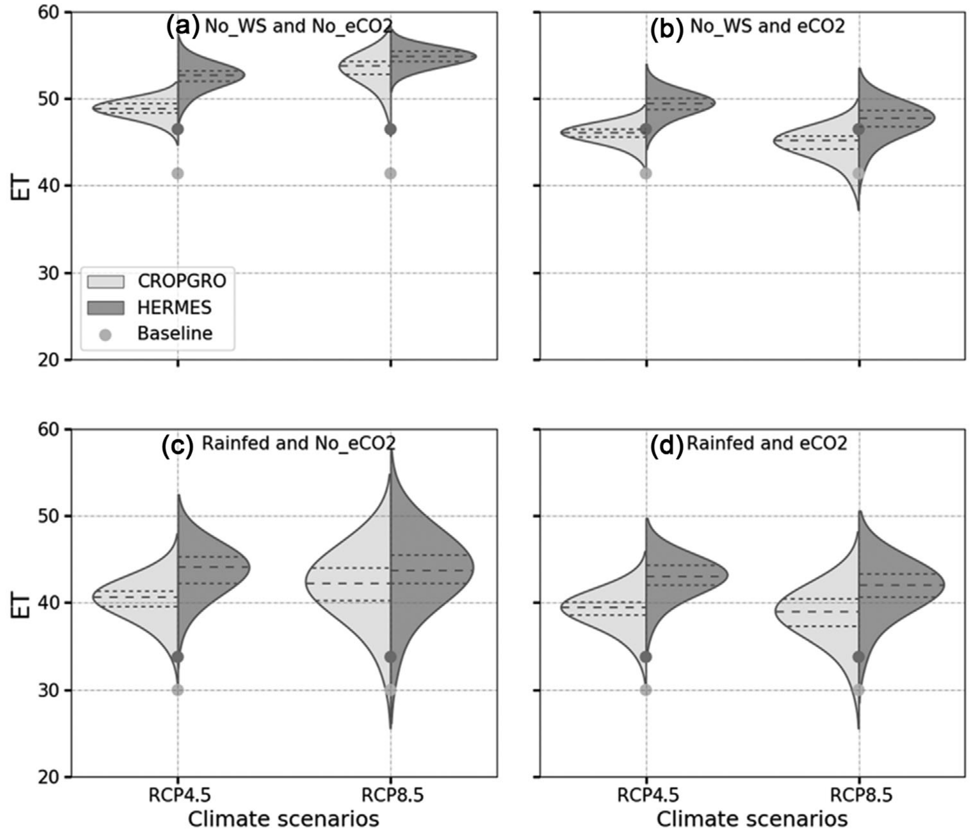

FIGURE 7 Violin distributions of simulated average seasonal evapotranspiration (ET, cm) from 2083 to 2099 for the 40 general circulation model (GCM) projections by CROPGRO (light gray) and HERMES (gray) in response to combined factors of water stress ([a and b] No_WS [Irrigation], and [c and d] Rainfed), temperature increase (2.5 ˚C for RCP4.5 and 4.5 ˚C for RCP8.5) and CO_2 levels (current CO_2 level: [a and c] No_eCO_2, [b and d] elevated CO_2 levels of 538 ppm for RCP4.5 and 936 ppm for RCP8.5: eCO_2). The baseline (dots) was averaged from the simulated soybean biomass under current climate condition from 2002 to 2017 with CO_2 level of 395 ppm. (The three insider lines from bottom to top in violin present the 25th, 50th, and 75th percentiles, respectively). Legend is applicable to all plots. RCP = Representative Concentration Pathways

reduced water stress by increased precipitation and elevated CO_2 (Table 4). Under irrigated conditions without CO_2 elevation, HERMES simulated greater decrease in biomass and seed yield compared to its baselines than CROPGRO (−19 to −26% vs. −3 to −9%), suggesting greater sensitivity to temperature increase in HERMES. Across the 40 GCM projections, both modules simulated higher variability among these GCMs under rainfed condition than irrigation conditions partly due to the greater variability in projected precipitation among the GCMs (Figure 2). Multiple crop models along with different GCMs can potentially reduce the uncertainty of the predicted climate change effects (Battisti et al., 2017; Maioranoa et al., 2017).

The variability of projected climate change effects on soybean production across the 40 GCM projections was lower for CROPGRO than for HERMES under irrigated conditions (e.g., Figures 3–6) and were similar under rainfed conditions. In addition, much higher variability in simulated biomass and yield was observed among years than among GCMs. These results were generally consistent with Asseng et al. (2013) and Wang et al. (2017), who found lower variability among different models than among GCMs, but high uncertainties in models under extreme climatic conditions.

The simulated reduction in soybean biomass and yield due to increased air temperature was associated more with the reduced leaf photosynthesis rate than shortened growing season in the two modules (Figure 2) (Ruiz-Vera et al., 2013). For example, with obviously earlier maturity date simulated by HERMES under RCP4.5 and RCP8.5 (Figure 8), higher soybean production relative to the baseline was with normal maturity date (Figures 3 and 4). This result was mainly due to the increased leaf photosynthesis rate with elevated CO_2 that compensated for the short growing season due to increased air temperature (Figure 2). Similar to previous climate change effect projections, only CO_2 effects on photosynthesis and transpiration were considered in the modules, and their effects on other physiological processes (i.e., phenology development) and interactions with high air temperature (i.e., on stomatal conductance and intercellular CO_2 concentration) should also be included (Castro et al., 2009; Ruiz-Vera et al., 2013).

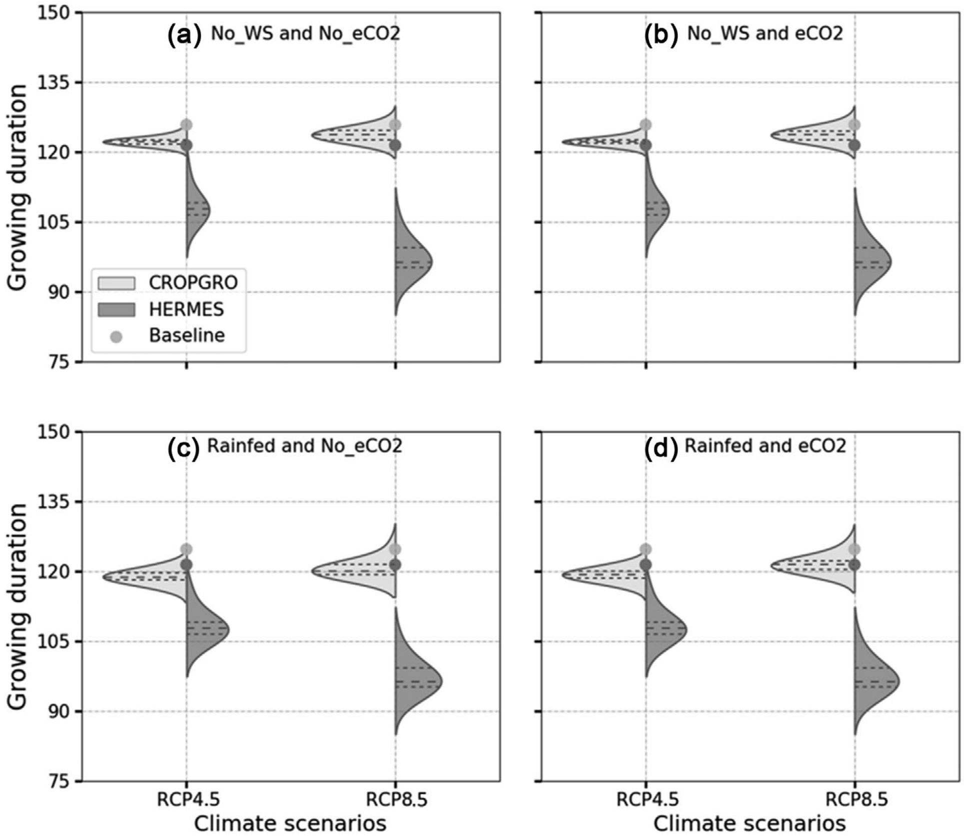

FIGURE 8 Violin distributions of simulated average soybean growing duration (days after planting, DAP) from 2083 to 2099 for the 40 general circulation model (GCM) projections by CROPGRO (light gray) and HERMES (gray) in response to combined factors of water stress ([a and b] No_WS [Irrigation], and [c and d] Rainfed), temperature increase (2.5 ˚C for RCP4.5 and 4.5 ˚C for RCP8.5) and CO_2 levels (current CO_2 level: [a and c] No_eCO_2, [b and d] elevated CO_2 levels of 538 ppm for RCP4.5 and 936 ppm for RCP8.5: eCO_2). The baseline (dots) was averaged from the simulated soybean growing duration under current climate condition from 2002 to 2017 with CO_2 level of 395 ppm. (The three insider lines from bottom to top in violins present the 25th, 50th, and 75th percentiles across the 40 GCM projections, respectively). Legend is applicable to all plots. RCP =Representative Concentration Pathways

Although there was much less increase in biomass and yield for both RCP4.5 and RCP8.5 under irrigated conditions compared to baselines, simulated biomass and yield were much higher and more stable than those under rainfed conditions (Table 4). Therefore, irrigation remained an effective mitigation strategy. On the other hand, neither module simulated sowing date effects (plus or minus 2 wk from current dates) on soybean production under both RCPs and under either rainfed or irrigation conditions, which might be caused by the GCM projections and calibrated crop parameters (Islam, Ahuja, Garcia, Ma, Saseendran, & Trout, 2012; Ma et al., 2017). However, shifting sowing dates by a month showed inconsistent results between the two modules. For example, without CO_2 fertilization effects under RCP4.5, advancing sowing date for 1 mo decreased soybean yield in both modules, but delaying it for 1 mo increased soybean yield by 10% in CROPGRO (19% at normal sowing date) and by 4% in HERMES (−7% at normal sowing date). Under RCP8.5, neither advancing nor delaying sowing dates was effective in mitigating climate change effects with yield decreasing by 11–31% compared to baseline scenarios.

The present model simulation may be specially associated with the cultivar parameters and local weather conditions used in this study, as genetic variation in the response of soybean to temperature increase has been reported (e.g., Kumagai & Sameshima, 2014; Salem, Kakani, Koti, & Reddy, 2007). More experiments with different cultivars and climate conditions are needed to evaluate the models and reduce the uncertainties associated with the crop parameters. Historical radiation and relative humidity data are used for model runs as they are not predicted by any of the GCMs; however, the interactions between temperature and radiation may affect the results (Malone et al., 2011; Mera, Niyogi, Buol, Wilkerson, & Semazzi, 2006). Furthermore, since both modules underpredicted soybean yield reduction (Sima et al., 2020), the projected yield decrease due to elevated air temperature may be under-estimated.

5 | CONCLUSIONS

Using 40 GCM projections and two crop modules (CROPGRO and HERMES) in RZWQM2, we demonstrated that soybean production would likely increase by 2100 under both RCP4.5 and RCP8.5 when considering CO_2 fertilization effects. Without CO_2 effects, soybean seed yield was simulated to decrease except for an increase of 19% in simulated rainfed yield by CROPGRO under RCP4.5. Simulated variability was higher under rainfed conditions than under irrigated conditions, higher among years than among GCMs, and higher by HERMES than by CROPGO. Due to much higher simulated yield under irrigation, supplementary irrigation may be an effective mitigation strategy to maintain soybean yield. In contrast, advancing or delaying sowing dates had little effect on soybean production in the region. Better phenology responses to temperature are needed in HERMES. Since both modules in RZWQM2 were calibrated with fully irrigated soybean data, further work is also needed to evaluate the responses of soybean growth to water stresses under elevated air temperature using experimental data to assure accurate simulation of the interactions between soil water content and air temperature.

ACKNOWLEDGMENTS

Q. X. Fang was supported in part by the National Natural Science Foundation of China (31671627).

CONFLICT OF INTEREST

The authors declare no conflict of interest.

ORCID

Q. X. Fang https://orcid.org/0000-0003-3720-6769

REFERENCES

Alagarswamy, G., Boote, K. J., Allen, L. H. Jr., & Jones, J. W. (2006). Evaluating the CROPGRO–Soybean model ability to simulate photosynthesis response to carbon dioxide levels. *Agronomy Journal*, *98*, 34–42. https://doi.org/10.2134/agronj2004-0298

Alexandrov, V., Eitzinger, J., Cajic, V., & Oberforster, M. (2002). Potential impact of climate change on selected agricultural crops in northeastern Austria. *Global Change Biology*, *8*, 372–389. https://doi.org/10.1046/j.1354-1013.2002.00484.x

Alexandrov, V. A., & Hoogenboom, G. (2000). Vulnerability and adaptation assessments of agricultural crops under climate change in the southeastern USA. *Theoretical and Applied Climatology*, *67*, 45–63. https://doi.org/10.1007/s007040070015

Asseng, S., Ewert, F., Rosenzweig, C., Jones, J. W., Hatfield, J. L., Ruane, A. C., & Brisson, N. (2013). Uncertainty in simulating wheat yields under climate change. *Nature Climate Change*, *3*, 827–832. https://doi.org/10.1038/nclimate1916

Bao, Y., Hoogenboom, G., McClendon, R., & Urich, P. (2015). Soybean production in 2025 and 2050 in the southeastern USA based on the SimCLIM and the CSM- CROPGRO-Soybean models. *Climate Research*, *63*, 73–89. https://doi.org/10.3354/cr01281

Bao, Y., Hoogenboom, G., McClendon, R. W., & Paz, J. O. (2015). Potential adaptation strategies for rainfed soybean production in the south-eastern USA under climate change based on the CSM-CROPGRO-Soybean model. *Journal of Agricultural Science*, *153*, 798–824. https://doi.org/10.1017/S0021859614001129

Balvanshi, A., & Tiwari, H. L. (2019). Mitigating future climate effects on wheat and soybean yields in central region of Madhya Pradesh by shifting sowing dates. *Journal of Agrometeorology*, *21*, 468–473.

Battisti, R., Sentelhas, P. C., & Boote, K. J. (2017). Inter-comparison of performance of soybean crop simulation models and their ensemble in southern Brazil. *Field Crops Research*, *200*, 28–37. https://doi.org/10.1016/j.fcr.2016.10.004

Battisti, R., Sentelhas, P. C., Park, P. S., Nendel, C., Camara, G. M. De S., Farias, J. R. B., & Basso, C. J. (2018). Assessment of crop-management strategies to improve soybean resilience to climate change in Southern Brazil. *Crop & Pasture Science*, *69*, 154–162. https://doi.org/10.1071/CP17293

Boote, K. J., Jones, J. W., & Hoogenboom, G. (1998). Simulation of crop growth: CROPGRO Model. In R M. Peart & R B. Curry (Eds.), *Agricultural systems modeling and simulation* (pp. 651–692). New York: Marcel Dekker.

Boote, K. J., & Pickering, N. B. (1994). Modeling photosynthesis of row crop canopies. *Hortscience*, *29*, 1423–1434. https://doi.org/10.21273/HORTSCI.29.12.1423

Brekke, L., Thrasher, B. L., Maurer, E. P., & Pruittt, T. (2013). *Downscaled CMIP3 and CMIP5 climate projections: Release of downscaled CMIP5 climate projections, comparison with preceding information, and summary of user needs*. Washington, DC: U.S. Department of the Interior, Bureau of Reclamation. Retrieved from http://gdo-dcp.ucllnl.org/downscaled_cmip_projections/techmemo/downscaled_climate.pdf

Carbone, G. J., Kiechle, W., Locke, C., Mearns, L. O., McDaniel, L., & Downton, M. W. (2003). Response of soybean and sorghum to varying spatial scales of climate change scenarios in the southeastern United States. *Climatic Change*, *60*, 73–98. https://doi.org/10.1023/A:1026041330889

Castro, J. C., Dohleman, F. G., Bernacchi, C. J., & Long, S. P. (2009). Elevated CO_2 significantly delays reproductive development of soybean under Free-Air Concentration Enrichment (FACE). *J. Exper. Botany*, *60*, 2945–2951.

Eulenstein, F., Lana, M., Schlindwein, S., Sheudzhen, A., Tauschke, M., Behrend, A., Guevara E., & Meira, S. (2017). Trends of soybean yields under climate change scenarios. *Hortculturae*, *3*(1), 10. https://doi.org/10.3390/horticulturae3010010

Fu, T., Ha, B., & Ko, J. (2016). Simulation of CO_2 enrichment and climate change impacts on soybean production. *International Agrophysics*, *30*, 25–37. https://doi.org/10.1515/intag-2015-0069

Hatfield, J. L., Boote, K. J., Kimball, B. A., Ziska, L. H., Izaurralde, R. C., Ort, D., … Wolfe, D. (2011). Climate impacts on agriculture: Implications for crop production. *Agronomy Journal*, *103*, 351–370. https://doi.org/10.2134/agronj2010.0303

Heinemann, A. B., de, H. N., Maia, A., Dourado-Neto, D., Ingram, K. T., & Googenboom, G. (2006). Soybean (*Glycine max* (L.) Merr.) growth and development response to CO_2 enrichment under different temperature regimes. *European Journal of Agronomy*, *24*, 52–61. https://doi.org/10.1016/j.eja.2005.04.005

IPCC. (2014). *Climate Change 2014: Synthesis Report Contribution of Working Groups I II and III to the Fifth Assessment Report of the Intergovernmental Panel on Climate Change* (Core Writing Team: R.K. Pachauri and L.A. Meyer [Eds.]). Geneva, Switzerland: IPCC. https://www.ipcc.ch/site/assets/uploads/2018/05/SYR_AR5_FINAL_full_wcover.pdf

Islam, A., Ahuja, L. R., Garcia, L. A., Ma, L., & Saseendran, S. A. (2012). Modelling effect of climate change and elevated CO_2 on potential evapotranspiration demand using multi-model ensemble climate change scenarios. *Transactions of the ASABE*, *55*, 2135–2146.

Islam, A., Ahuja, L. R., Garcia, L. A., Ma, L., Saseendran, S. A., & Trout, T. J. (2012). Modelling the impact of climate change on corn yield using multi-model ensemble climate change scenarios. *Agricultural Water Management*, *110*, 94–108. https://doi.org/10.1016/j.agwat.2012.04.004

Jin, Z., Ainsworth, E. A., Leakey, A. D. B., & Lobell, D. B. (2018). Increasing drought and diminishing benefits of elevated carbon dioxide for soybean yields across the US Midwest. *Global Change Biology*, *24*, e522–e533. https://doi.org/10.1111/gcb.13946

Jing, Q., Huffman, T., Shang, J., Liu, J., Pattey, E., Morrison, M., … Qian, B. (2017). Modelling soybean yield responses to seeding date under projected climate change scenarios. *Canadian Journal of Plant Science*, *97*, 1152–1164.

Jones, J. W., Hoogenboom, G., Porter, C. H., Boote, K. J., Batchelor, W. D., Hunt, L. A., … Ritchief, J. T. (2003). The DSSAT cropping system model. *European Journal of Agronomy*, *18*, 235–265. https://doi.org/10.1016/S1161-0301(02)00107-7

Kersebaum, K. C. (1995). Application of a simple management model to simulate water and nitrogen dynamics. *Ecological Modelling*, *81*, 145–156. https://doi.org/10.1016/0304-3800(94)00167-G

Kersebaum, K. C. (2013). Temperature driven processes in the crop module of the HERMES model. In P. D. Alderman, E. Quilligan, S. Asseng, F. Ewert, and M. P. Reynolds (Eds.), *Proceedings of the Workshop on Modeling Wheat Response to High Temperature. CIMMYT, El 19–21 June 2013, Batán, Mexico* (pp. 66–69). Mexico, DF: CIMMYT. Retrieved from https://repository.cimmyt.org/handle/10883/3211

Kersebaum, K. C., & Nendel, C. (2014). Site-specific impacts of climate change on wheat production across regions of Germany using different CO_2 response functions. *European Journal of Agronomy*, *52*, 22–32. https://doi.org/10.1016/j.eja.2013.04.005

Kumagai, E., & Sameshima, R. (2014). Genotypic differences in soybean yield responses to increasing temperature in a cool climate are related to maturity group. *Agricultural and Forest Meteorology*, *198–199*, 265–272. https://doi.org/10.1016/j.agrformet.2014.08.016

Lal, M., Singh, K. K., Srinivasan, G., Rothore, L. S., Naidu, D., & Tripathi, C. N. (1999). Growth and yield responses of soybean in Madhya Pradesh, India to climate variability and change. *Agricultural and Forest Meteorology*, *93*, 53–70. https://doi.org/10.1016/S0168-1923(98)00105-1

Long, S. P. (1991). Modification of the response of photosynthetic productivity to rising temperature by atmospheric CO_2 concentrations–Has its importance been underestimated? *Plant, Cell and Environment*, *14*, 729–739. https://doi.org/10.1111/j.1365-3040.1991.tb01439.x

Ma, L., Ahuja, L. R., Islam, A., Trout, T. J., Saseendran, S. A., & Malone, R. W. (2017). Modeling yield and biomass responses of maize cultivars to climate change under full and deficit irrigation. *Agricultural Water Management*, *180*, 88–98. https://doi.org/10.1016/j.agwat.2016.11.007

Ma, L., Ahuja, L. R., Nolan, B. T., Malone, R. W., Trout, T. J., & Qi, Z. (2012). Root Zone Water Quality Model (RZWQM2): Model use, calibration and validation. *Transactions of the ASABE*, *55*, 1425–1446. https://doi.org/10.13031/2013.42252

Ma, L., Hoogenboom, G., Ahuja, L. R., Nielsen, D. C., & Ascough II J. C. (2005). Development and evaluation of RZWQM-CROPGRO hybrid model for soybean production. *Agronomy Journal*, *97*, 1172–1182. https://doi.org/10.2134/agronj2003.0314

Maiorano, A., Martre, P., Asseng, S., Ewert, Frank, Muller, C., Rotter, R. P., Ruane, A. C., … Zhu, Y. (2017). Crop model improvement reduces the uncertainty of the response to temperature of multi-model ensembles. *Field Crops Research*, *202*, 5–20. https://doi.org/10.1016/j.fcr.2016.05.001

Mall, R. K., Lal, M., Bahatia, V. S., Rathore, L. S., & Singh, R. (2004). Mitigating climate change impact on soybean productivity in India: A simulation study. *Agricultural and Forest Meteorology*, *121*, 113–125. https://doi.org/10.1016/S0168-1923(03)00157-6

Malone, R. W., Meek, D., Ma, L., Jaynes, D., Nolan, B. T., & Karlen, D. (2011). Quality control of weather data for agricultural system model input. In L. R. Ahuja & L. Ma (Eds.), *Methods of introducing system models into agricultural research* (pp. 283–295). ASA, CSSA, SSSA

Meinshausen, M., Smith, S. J., Calvin, K., Daniel, J. S., Kainuma, M. L. T., Lamarque, J.-F., … van Vuuren, D. P. P. (2011). The RCP greenhouse gas concentrations and their extensions from 1765 to 2300. *Climatic Change*, *109*, 213–241. https://doi.org/10.1007/s10584-011-0156-z

Mera, R. J., Niyogi, D., Buol, G. S., Wilkerson, G. G., & Semazzi, F. H. M. (2006). Potential individual versus simultaneous climate change effects on soybean (C3) and maize (C4) crops: An agrotechnology model based study. *Global and Planetary Change*, *54*, 163–182. https://doi.org/10.1016/j.gloplacha.2005.11.003

Mitchell, R. A. C., Lawlor, D. W., Mitchell, V. J., Gibbard, C. L., White, E. M., & Porter, J. R. (1995). Effects of elevated CO_2 concentration and increased temperature on winter wheat–Test of ARCWHEAT1 simulation model. *Plant, Cell and Environment*, *18*, 736–748. https://doi.org/10.1111/j.1365-3040.1995.tb00576.x

Nendel, C., Kersebaum, K. C., Mirschel, W., Manderscheid, R., Weigel, H. J., &Wendel, K. O. (2009). Testing different CO_2 response algorithms against a FACE crop rotation experiment. *NJAS - Wageningen Journal of Life Sciences*, *57*, 17–25. https://doi.org/10.1016/j.njas.2009.07.005

Pickering, N. B., Jones, J. W., & Boote, K. J. (1995). Adapting SOYGRO V5.42 for prediction under climate change conditions. (pp. 77–98). In C. Rosenzweig, et al. (Eds.), *Climate change and Agriculture: Analysis of potential international impacts*. Madison, WI: ASA Spec. Publ. 59. ASA, CSSA, and SSSA.

Pierce, D. W., Cayan, D. R., Maurer, E. P., Abatzoglou, J. T., & Hegewisch, K. C. (2015). Improved bias correction techniques for hydrological simulations of climate change. *Journal of Hydrometeorology*, *16*, 2421–2442. https://doi.org/10.1175/JHM-D-14-0236.1

Rawls, W. J., Brakensiek, D. L., & Saxton, K. E. (1982). Estimation of soil water properties. *Transactions of the ASAE*, *25*, 1316–1320. https://doi.org/10.13031/2013.33720.

Rolla, A. L., Nunez, M. N., Guevara, E. R., Meira, S. G., Rodriguez, G. R., & de Zarate, M. I. O. (2018). Climate impacts on crop yields in central Argentina, adaptation strategies. *Agricultural Systems*, *160*, 44–59. https://doi.org/10.1016/j.agsy.2017.08.007

Ruiz-Nogueira, B., Boote, K. J., & Sau, F. (2001). Calibration and use of CROPGRO- Soybean model for improving soybean management under rainfed conditions in Galicia Northwest Spain. *Agricultural Systems*, *68*, 151–173. https://doi.org/10.1016/S0308-521X(01)00008-7

Ruiz-Vera, U. M., Siebers, Matthew, Gray, Sharon B., Drag, David W., Rosenthal, David M., Kimball, Bruce A., Ort, D. R., & Bernacchi, Carl J. (2013). Global warming can negate the expected CO_2 stimulation in photosynthesis and productivity for soybean grown in the midwestern United States. *Plant Physiology*, *162*, 410–423. https://doi.org/10.1104/pp.112.211938

Salem, M. A., Kakani, V. G., Koti, S., & Reddy, K. R. (2007). Pollen-based screening of soybean genotypes for high temperatures. *Crop Science*, *47*, 219–231. https://doi.org/10.2135/cropsci2006.07.0443

Schauberger, B., Archontoulis, S., Arneth, A., Balkovic, J., Ciais, P., Deryng, D., & Pugh, T. A. (2017). Consistent negative response of US crops to high temperatures in observations and crop models. *Nature Communications*, *8*, 13931. https://doi.org/10.1038/ncomms13931

Sima, M. W., Fang, Q. X., Burkey, K. O., Ray, S. J., Pursley, W. A., Kersebaum, K. C., Boote, K. J., & Malone, R. W. (2020). Field and model assessments of irrigated soybean responses to increased air temperature. *Agronomy Journal*, *112*(6), 4849–4860. https://doi.org/10.1002/agj2.20394

Sohoulande, C. D. D., & Singh, V. P. (2016). Impact of climate change on precipitation patterns: A comparative approach. *International Journal of Climatology*, *36*, 3588–3606. https://doi.org/10.1002/joc.4578

Sohoulande, C. D. D., Stone, K., Szogi, A., & Bauer, P. (2019). An investigation of seasonal precipitation patterns for rainfed agriculture in the southeastern region of the United States. *Agricultural Water Management*, *223*, 105728. https://doi.org/10.1016/j.agwat.2019.105728

Wang, Z., Qi, Z., Xue, L., Bukovsky, M., & Helmers, M. J. (2015). Modeling the impacts of climate change on nitrogen losses and crop yield in a subsurface drained field. *Climatic Change*, *129*, 323–335. https://doi.org/10.1007/s10584-015-1342-1

Wang, E., Martre, P., Zhao, Z., Ewert, F., et al. (2017). The uncertainty of crop yield projections is reduced by improved temperature response functions. *Nature Plants*, *3*, 17102. https://doi.org/10.1038/nplants.2017.102

Wolf, J. (2002a). Comparison of two soya bean simulation models under climate change: Model calibration and sensitivity analyses. *Climate Research*, *20*, 56–70.

Wolf, J. (2002b). Comparison of two soya bean simulation models under climate change: Application of climate change scenarios. *Climate Research*, *20*, 71–81. https://doi.org/10.3354/cr020071

How to cite this article: Ma L, Fang QX, Sima MW, Burkey KO, Harmel RD. Simulated climate change effects on soybean production using two crop modules in RZWQM2. *Agronomy Journal*. 2021;*113:*1349–1365. https://doi.org/10.1002/agj2.20548